Isı Bilimi ve Tekniği Dergisi, 30, 2, 09-19, 2010
J. of Thermal Science and Technology

ISSN 1300-3615

OPTIMIZATION OF STRAIGHT FINS WITH A STEP CHANGE IN THICKNESS AND VARIABLE THERMAL CONDUCTIVITY BY HOMOTOPY PERTURBATION METHOD

Cihat ARSLANTÜRK
Department of Mechanical Engineering, Faculty of Engineering, Ataturk University, 25240 Erzurum, Turkey
e-mail : carslan@atauni.edu.tr

(Geliş Tarihi: 08. 07. 2009, Kabul Tarihi: 03. 11. 2009)

Abstract: For the better utilization of fin material, it is proposed a modified geometry of new fin with a step change in thickness (SF) in the literature. In the present paper, the thermal analysis and optimization of convective straight fins with a step change in thickness and temperature-dependent thermal conductivity have been addressed. Temperature distribution within the fin has been evaluated using homotopy perturbation method (HPM) which provides an analytical solution in the form of an infinite power series. The optimum geometry which maximizes the heat transfer rate for a given fin volume has been found by using the data from the solution. It has been observed that a SF is the better choice for transferring rate of heat in comparison with the flat fins for the same fin volume and identical thermal conditions. The derived condition of optimality gives an open choice to the designer.

Keywords: Fin, Homotopy perturbation method, Optimization, Variable conductivity.

ISIL İLETKENLİĞİ SICAKLIKLA DEĞİŞEN KADEMELİ KANATLARIN HOMOTOPİ PERTÜRBASYON YÖNTEMİ İLE OPTİMİZASYONU

Özet: Kanat malzemesinin verimli kullanılabilmesi için kademeli kanat olarak isimlendirilen yeni bir kanat geometrisi önerilmiştir. Bu çalışmada, ısıl iletkenliği sıcaklıkla değişen dikdörtgen kesitli kademeli kanatların ısıl analizi ve optimizasyonu yapılmıştır. Kanat içindeki sıcaklık dağılımı, sonsuz kuvvet serisi şeklinde analitik bir çözüm sağlayan Homotopi Pertürbasyon Metodu (HPM) ile elde edilmiştir. Bu çözüm, verilen sabit bir kanat hacmi için ısı geçişini maksimum yapan kanat geometrisinin bulunması için kullanılmıştır. Elde edilen sonuçlar, aynı ısıl koşullar ve aynı kanat hacmi için kademeli kanadın düz kanada göre daha fazla ısı geçişi sağladığını göstermiştir. Optimizasyondan elde edilen sonuçlar, bu tip kanatların tasarımı için kullanılabilir.

Anahtar Kelimeler: Kanat, Homotopi pertürbasyon yöntemi, Optimizasyon, Değişken ısı iletim katsayısı.

NOMENCLATURE

a	dimensionless cross-sectional area ($=A_c/2L^2$)
A	general differential operator
A_c	cross-sectional area of the fin (m^2)
B	boundary operator
Bi	Biot number ($=hL/k_\infty$)
$C_{1,2,3}$	integral constants
h	heat transfer coefficient [$W/(m^2K)$]
k	thermal conductivity [W/(mK)]
ℓ	length of the thin section of the fin (m)
L	linear operator or length of the entire fin (m)
N	nonlinear operator
p	homotopy parameter
q	dimensionless heat transfer rate [$=Q/2k_\infty(T_b-T_\infty)$]
Q	heat transfer rate per unit fin depth (W/m)
t	unreduced semi-thickness of the fin (m)
T_1	temperature within the thin section (K)
T_2	temperature within the thick section (K)
T_b	base temperature, (K)
T_∞	ambient fluid temperature, (K)
x	axial coordinate for entire fin, (m)
x_1	axial coordinate for the thin section (m)
x_2	axial coordinate for the thick section (m)

Greek symbols

α	thickness parameter
β	thermal conductivity parameter [=κ(T_b-T_∞)]
δ	dimensionless fin semi thickness
κ	the slope of the thermal conductivity-temperature curve (1/K)
λ	length ratio (=ℓ /L)
θ	dimensionless temperature within the thin section of the fin [=(T_1-T_∞)/(T_b-T_∞)]
ϕ	dimensionless temperature within the thick section of the fin [=(T_2-T_∞)/(T_b-T_∞)]
ξ	dimensionless axial coordinate of the thin section of the fin (=x_1/L)
τ	dimensionless axial coordinate of the thick section of the fin (=x_2/L)
ζ	dimensionless axial coordinate for the entire fin (=x/L)

INTRODUCTION

Fins or extended surfaces are frequently used in heat transfer equipments to increase the surface area, and, consequently, to augment the rate of heat transfer between the primary surface and surrounding fluid. The selection of any particular type of fin depends mainly on the geometry of the primary surface (Kundu and Das, 2007). An accurate analysis of heat transfer in fins has become crucial with the growing demand of high performance of heat transfer surfaces with progressively smaller weights, volumes, initial and running cost of the system. Over the years different fin shapes have been evolved depending upon the application and the geometry of the primary surface. Kern and Kraus (1972) have identified three main fin geometries. These are longitudinal fins, radial or circumferential fins and pin fins or spines. For any of the above geometry, fins with straight profile or constant thickness are a common choice as they can be manufactured easily. The thermal design of a constant thickness fin is also relatively simple. However, in any fin the temperature difference reduces from the fin base to fin tip. Accordingly, a saving of fin material can be obtained by progressively narrowing down the fin section. This has initiated a lot of exercises for the determination of optimum fin shapes so that the fin volume is minimum for a given rate of heat dissipation or the rate of heat dissipation is maximum for a given fin volume (Kundu and Das, 2002). Hollands and Stedman (1992) proposed a design of absorber plate fin with a step reduction in thickness towards the fin tip for saving in fin material. The results from this study indicate that roughly a 20 % reduction in fin material is possible. Aziz (1994) investigated the optimum dimensions of convective rectangular fins with a step change in cross-sectional area. A similar profile has also been adopted for radial fins by Kundu and Das (Kundu and Das, 2001). Malekzadeh et al. (2006) used the differential quadrature method for optimization of convective-radiative flat and step fins . Recently, Kundu (2009) analyzed an annular fin with a step change in thickness under fully and partially wet surface conditions. The optimization study demonstrated that an annular fin with a step change in thickness is the better choice for transferring rate of heat in comparison with the concentric-annular disc fin for the same fin volume and identical surface conditions (Kundu, 2009).

In the present work, the convective straight fins with a step change in thickness and temperature-dependent thermal conductivity have been considered for the better utilization of fin material. Since the fin has a step change in thickness, the fin problem has been divided into two parts as thin and thick sections. Resulting two nonlinear heat transfer equations with nonlinear boundary conditions have been solved by HPM, which is used for solving various nonlinear fin problems, to obtain the fin temperature distribution. Employing the temperature distribution, the heat transfer rate has been evaluated. The main problem is to maximize the heat transfer rate for a given fin volume, thermal conductivity parameter, β, and Biot number, Bi. The optimization variables are of thickness parameter, α, and fin length ratio, λ. Optimum geometrical parameters and maximum heat transfer rates for various combinations of thermal and geometrical parameters are presented to provide an open choice to the designer.

PROBLEM DESCRIPTION

Fig. 1 schematically depicts a straight step fin. The fin has a constant thickness 2αt (0<α<1) from the fin tip up to x_1=ℓ, beyond that the fin thickness is 2t up to fin base.

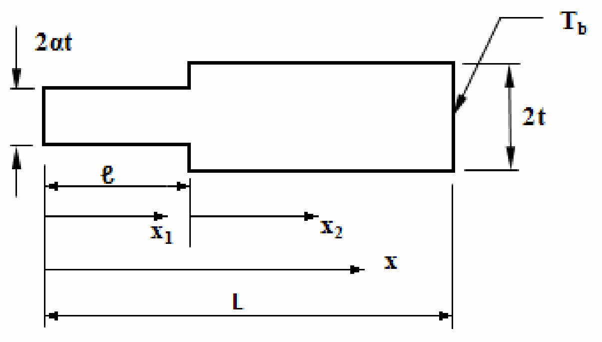

Figure 1. Schematic of a convective fin with a step change in thickness.

The mathematical model in the problem is based on some assumptions:

1. The temperature distribution and heat transfer are steady.
2. The fin material is homogeneous and isotropic.
3. Only the convection effects between the fin surfaces and surroundings are considered.

4. The fin conductivity varies with temperature linearly.
5. The heat coefficient overall the fin surfaces are the same.
6. The surrounding temperature, T_∞, is uniform.
7. The temperature of the fin base, T_b, is uniform.
8. The fin thickness is far smaller than its length that the temperature gradient normal to its surface can be neglected.
9. The heat transfer from the fin tip is negligible.

For each part of the fin, energy balance equations are given as:

$$2\alpha t\frac{d}{dx_1}\left[k(T_1)\frac{dT_1}{dx_1}\right]-2h(T_1-T_\infty)=0 \tag{1a}$$

$$2t\frac{d}{dx_2}\left[k(T_2)\frac{dT_2}{dx_2}\right]-2h(T_2-T_\infty)=0 \tag{1b}$$

Invoking the continuity of temperature and heat current at the junction, boundary conditions of the governing equations can be expressed as:

$$\left.\frac{dT_1}{dx_1}\right|_{x_1=0}=0 \tag{1c}$$

$$T_1(\ell)=T_2(0) \tag{1d}$$

$$\left[k\frac{dT_2}{dx_2}\right]_{x_2=0}-(1-\alpha)h\left[T_2-T_\infty\right]_{x_2=0}=\left[\alpha k\frac{dT_1}{dx_1}\right]_{x_1=\ell} \tag{1e}$$

$$T_2(L-\ell)=T_b \tag{1f}$$

The thermal conductivity of the fin material is assumed to be a linear function of temperature according to $k(T)=k_\infty[1+\kappa(T-T_\infty)]$.

Where, k_∞ is the thermal conductivity at the ambient fluid temperature of the fin, κ is the parameter describing the variation of thermal conductivity. In order to simplify the parameter studies, the following non-dimensional variables are defined:

$$\xi=\frac{x_1}{L}\quad \tau=\frac{x_2}{L}\quad \lambda=\frac{\ell}{L}\quad \delta=\frac{t}{L}\quad Bi=\frac{hL}{k_\infty}$$
$$\theta=\frac{T_1-T_\infty}{T_b-T_\infty}\quad \phi=\frac{T_2-T_\infty}{T_b-T_\infty}\quad \beta=\kappa(T_b-T_\infty) \tag{2}$$

By using the aforementioned non-dimensional variables, the governing equations and their associated boundary conditions become as follows:

$$\frac{d^2\theta}{d\xi^2}+\beta\left(\frac{d\theta}{d\xi}\right)^2+\beta\theta\frac{d^2\theta}{d\xi^2}-\frac{Bi}{\alpha\delta}\theta=0,\quad 0<\xi<\lambda \tag{3a}$$

$$\frac{d^2\phi}{d\tau^2}+\beta\left(\frac{d\phi}{d\tau}\right)^2+\beta\phi\frac{d^2\phi}{d\tau^2}-\frac{Bi}{\delta}\phi=0,\quad 0<\tau<1-\lambda \tag{3b}$$

$$\left.\frac{d\theta}{d\xi}\right|_{\xi=0}=0 \tag{3c}$$

$$\theta(\lambda)=\phi(0) \tag{3d}$$

$$\left[(1+\beta\phi)\frac{d\phi}{d\tau}\right]_{\tau=0}-\left[(1-\alpha)Bi\phi\right]_{\tau=0}=\left[\alpha(1+\beta\theta)\frac{d\theta}{d\xi}\right]_{\xi=\lambda} \tag{3e}$$

$$\phi(1-\lambda)=1 \tag{3f}$$

HOMOTOPY PERTURBATION METHOD

The homotopy perturbation method was first proposed by the Chinese mathematician J. Huan He (He, 1999; He, 2000, He, 2003). This technique has been employed to solve a large variety of linear and nonlinear problems (Saadatmandi et al., 2009; Öziş and Ağırseven, 2008; Cowdhury and Hashim, 2008; Cowdhury and Hashim, 2009). The solution of a delay differential equation is presented by means of a homotopy perturbation method (Saadatmandi, 2009). A nonlinear convective–radiative cooling equation, a nonlinear heat equation (porous media equation) and a nonlinear heat equation with cubic nonlinearity are solved via this procedure (Öziş and Ağırseven, 2008). Analytical solutions by homotopy-perturbation method are implemented for solving the nonlinear heat transfer equations (Cowdhury and Hashim, 2008). This method is also adopted for solving pure strongly nonlinear second-order differential equations (Cowdhury and Hashim, 2009).

To illustrate the basic ideas of this method, we consider the following general nonlinear differential equation [9],

$$A(u)-f(r)=0\quad r\in\Omega \tag{4}$$

with boundary conditions

$$B(u,\partial u/\partial n)=0\quad r\in\Gamma, \tag{5}$$

where A is a general differential operator, B is a boundary operator, f(r) is a known analytic function, and Γ is the boundary of the domain Ω.

The operator A can be generally divided into linear and nonlinear parts say L and N. Therefore Equation (4) can be written as

$$L(u) + N(u) - f(r) = 0 \tag{6}$$

We construct a homotopy $\upsilon(r,p): \Omega \times [0,1] \rightarrow \Re$ which satisfies

$$H(\upsilon, p) = L(\upsilon) - L(u_0) + pL(u_0) + p[N(\upsilon) - f(r)] = 0 \tag{7}$$

where p is called homotopy parameter.

According to the HPM, the approximation solution of Equation (7) can be expressed as a series of the powers of p, i.e.

$$u = \lim_{p \to 1} \upsilon = \upsilon_0 + \upsilon_1 + \upsilon_2 \cdots. \tag{8}$$

THE FIN TEMPERATURE DISTRIBUTION

Following homotopy perturbation method to Equation (3a), linear and non-linear parts are defined as:

$$L(\theta) = \frac{d^2\theta}{d\xi^2} \tag{9}$$

$$N(\theta) = \beta\theta\frac{d^2\theta}{d\xi^2} + \beta\left(\frac{d\theta}{d\xi}\right)^2 - \psi^2\theta \tag{10}$$

where, $\psi^2 = \dfrac{Bi}{\alpha\delta}$.

Let $\dfrac{d\theta(0)}{d\xi} = 0$ from the Eq. (3c), together with $\theta(0) = C_1$, then we have:

$$\frac{d\theta}{d\xi} = 0 \quad \text{at} \quad \xi = 0, \qquad \theta = C_1 \quad \text{at} \quad \xi = 0 \tag{11}$$

Substituting Eq. (8) into Eq. (9) and then into Eq. (7) and rearranging based on power of p-terms we have:

p^0 :

$$\frac{d^2\theta_0}{d\xi^2} = 0 \tag{12a}$$

$$\frac{d\theta_0}{d\xi} = 0 \quad \text{at} \quad \xi = 0, \quad \theta_0 = C_1 \quad \text{at} \quad \xi = 0 \tag{12b}$$

p^1 :

$$\frac{d^2\theta_1}{d\xi^2} + \beta\left[\left(\frac{d\theta_0}{d\xi}\right)^2 + \theta_0\frac{d^2\theta_0}{d\xi^2}\right] - \psi^2\theta_0 = 0 \tag{13a}$$

$$\frac{d\theta_1}{d\xi} = 0 \quad \text{at} \quad \xi = 0, \qquad \theta_1 = 0 \quad \text{at} \quad \xi = 0 \tag{13b}$$

p^2 :

$$\frac{d^2\theta_2}{d\xi^2} + \beta\left[2\frac{d\theta_0}{d\xi}\frac{d\theta_1}{d\xi} + \theta_1\frac{d^2\theta_0}{d\xi^2} + \theta_0\frac{d^2\theta_1}{d\xi^2}\right] - \psi^2\theta_1 = 0 \tag{14a}$$

$$\frac{d\theta_2}{d\xi} = 0 \quad \text{at} \quad \xi = 0, \qquad \theta_2 = 0 \quad \text{at} \quad \xi = 0 \tag{14b}$$

p^3 :

$$\frac{d^2\theta_3}{d\xi^2} + \beta\left[2\frac{d\theta_0}{d\xi}\frac{d\theta_2}{d\xi} + \left(\frac{d\theta_1}{d\xi}\right)^2 + \theta_2\frac{d^2\theta_0}{d\xi^2} + \theta_1\frac{d^2\theta_1}{d\xi^2} + \theta_0\frac{d^2\theta_2}{d\xi^2}\right] - \psi^2\theta_2 = 0 \tag{15a}$$

$$\frac{d\theta_3}{d\xi} = 0 \quad \text{at} \quad \xi = 0, \quad \theta_3 = 0 \quad \text{at} \quad \xi = 0 \tag{15b}$$

p^4 :

$$\frac{d^2\theta_4}{d\xi^2} + \beta\left[2\frac{d\theta_1}{d\xi}\frac{d\theta_2}{d\xi} + 2\frac{d\theta_0}{d\xi}\frac{d\theta_3}{d\xi} + \theta_3\frac{d^2\theta_0}{d\xi^2} + \theta_2\frac{d^2\theta_1}{d\xi^2} + \theta_1\frac{d^2\theta_2}{d\xi^2} + \theta_0\frac{d^2\theta_3}{d\xi^2}\right] - \psi^2\theta_3 = 0 \tag{16a}$$

$$\frac{d\theta_4}{d\xi} = 0 \quad \text{at} \quad \xi = 0, \qquad \theta_4 = 0 \quad \text{at} \quad \xi = 0 \tag{16b}$$

$\vdots$

By increasing the number of the terms in the solution, higher accuracy will be obtained. Solving Eqs. (12a), (13a), (14a), (15a), (16a), we have θ_0, θ_1, θ_2, θ_3, and θ_4. When $p \rightarrow 1$, we have the solution for taking first five terms in the series as follows.

$$\begin{aligned}\theta(\xi) = C_1 &+ \frac{\Psi C_1^4}{2}\left(\beta^4C_1^4 - \beta^3C_1^3 + \beta^2C_1^2 - \beta C_1 + 1\right)\xi^2 \\ &+ \frac{\Psi^2C_1^7}{24}\left(-34\beta^3C_1^3 + 21\beta^2C_1^2 - 11\beta C_1 + 4\right)\xi^4 \\ &+ \frac{\Psi^3C_1^{10}}{720}\left(645\beta^2C_1^2 - 228\beta C_1 + 52\right)\xi^6 + \frac{\Psi^4C_1^{13}}{10080} \\ &\left(-1999\beta C_1 + 322\right)\xi^8 + \frac{929\Psi^5C_1^{16}}{64800}\xi^{10}\end{aligned}$$

Letting $\Omega^2 = \dfrac{Bi}{\delta}$, $\phi(0) = C_2$, $\dfrac{d\phi(0)}{d\eta} = C_3$ and applying the same procedure to Equation (3b), it can be written as follows:

p^0 :

$$\frac{d^2\phi_0}{d\tau^2}=0 \tag{17a}$$

$$\phi_0 = C_2 \quad \text{at} \quad \tau=0, \quad \frac{d\phi_0}{d\tau}=C_3 \quad \text{at} \quad \tau=0 \tag{17b}$$

p^1 :

$$\frac{d^2\phi_1}{d\tau^2}+\beta\left[\left(\frac{d\phi_0}{d\tau}\right)^2+\phi_0\frac{d^2\phi_0}{d\tau^2}\right]-\Omega^2\phi_0=0 \tag{18a}$$

$$\phi_1 = 0 \quad \text{at} \quad \tau=0, \quad \frac{d\phi_1}{d\tau}=0 \quad \text{at} \quad \tau=0 \tag{18b}$$

p^2 :

$$\frac{d^2\phi_2}{d\tau^2}+\beta\left[2\frac{d\phi_0}{d\tau}\frac{d\phi_1}{d\tau}+\phi_1\frac{d^2\phi_0}{d\tau^2}+\phi_0\frac{d^2\phi_1}{d\tau^2}\right] -\Omega^2\phi_1=0 \tag{19a}$$

$$\phi_2 = 0 \quad \text{at} \quad \tau=0, \quad \frac{d\phi_2}{d\tau}=0 \quad \text{at} \quad \tau=0 \tag{19b}$$

p^3 :

$$\frac{d^2\phi_3}{d\tau^2}+\beta\left[2\frac{d\phi_0}{d\tau}\frac{d\phi_2}{d\tau}+\left(\frac{d\phi_1}{d\tau}\right)^2+\phi_2\frac{d^2\phi_0}{d\tau^2}+ \phi_1\frac{d^2\phi_1}{d\tau^2}+\phi_0\frac{d^2\phi_2}{d\tau^2}\right]-\Omega^2\phi_2=0 \tag{20a}$$

$$\phi_3 = 0 \quad \text{at} \quad \tau=0, \quad \frac{d\phi_3}{d\tau}=0 \quad \text{at} \quad \tau=0 \tag{20b}$$

p^4 :

$$\frac{d^2\phi_4}{d\tau^2}+\beta\left[2\frac{d\phi_1}{d\tau}\frac{d\phi_2}{d\tau}+2\frac{d\phi_0}{d\tau}\frac{d\phi_3}{d\tau}+\phi_3\frac{d^2\phi_0}{d\tau^2} +\phi_2\frac{d^2\phi_1}{d\tau^2}+\phi_1\frac{d^2\phi_2}{d\tau^2}+\phi_0\frac{d^2\phi_3}{d\tau^2}\right]-\Omega^2\phi_3=0 \tag{21a}$$

$$\phi_4 = 0 \quad \text{at} \quad \tau=0, \quad \frac{d\phi_4}{d\tau}=0 \quad \text{at} \quad \tau=0 \tag{21b}$$

$\vdots$

Solving Eqs. (17a),(18a), (19a),(20a), (21a), we have we have ϕ_0, ϕ_1, ϕ_2, ϕ_3, and ϕ_4. When $p\rightarrow 1$,we have the solution for taking first five terms in the series as follows.

$$\begin{aligned}\phi(\eta) &= C_2 + C_3\tau + \frac{1}{2}\Big[\Omega\big(C_2^4 - C_2^5\beta + C_2^6\beta^2 - C_2^7\beta^3 + C_2^8\beta^4\big) - \beta C_3^2 + \beta^2 C_3^2 C_2 - \beta^3 C_3^2 C_2^2 + \beta^4 C_3^2 C_2^3 \\ &\quad - \beta^5 C_3^2 C_2^4\Big]\tau^2 + \Big[\frac{1}{6}\Omega C_3\big(4C_2^3 - 7\beta C_2^4 + 10\beta^2 C_2^5 - 13\beta^3 C_2^6 + 16\beta^4 C_2^7\big) + \frac{1}{2}\beta^3 C_3^3\big(1 - 2\beta C_2 \\ &\quad + 3\beta^2 C_2^2 - 4\beta^3 C_2^3\big)\Big]\tau^3 + \cdots\end{aligned} \tag{22}$$

Integration constant C_1 represents the temperature at the fin tip. C_2, and C_3 are temperature and temperature gradient at the cross-section where the step change in thickness occurs, respectively. The constants can be evaluated from the boundary conditions given in Equations (3d)-(3f) using classical Newton-Raphson method.

CONVERGENCE AND ACCURACY OF THE SERIES SOLUTION

Table 1 shows the dimensionless tip temperature as a function of the number of terms in the series for different thermal conductivity parameters, β. The impact of the number of terms in the series solution, and the series truncation process, are assessed by evaluating the homotopy perturbation results for the case of the strongest nonlinearity with 1–10 terms in the series. The table states that the convergence of the solution for the higher absolute value of the thermal conductivity parameter is faster than the solution with lower value of conductivity parameter. It can be observed from the figure that the difference between adjacent terms remains quite small as the number of terms, n, increases. As n > 9, the maximum difference never exceeds 0.2 %. Theoretically we should calculate a great number of terms to match the analytical solution but as a matter of fact, when we obtain ten terms of approximate solution is reached, the outcomes attain to a very good accuracy.

If β=0, Eqs. (3a) and (3b) will become a set of linear differential equations and it has an analytic solution:

$$\theta(\xi)=\frac{\cosh(m_1\xi)}{\cosh(\omega_1)}\theta_j \tag{23a}$$

$$\phi(\xi)=\theta_j\cosh(m_2\tau)+\frac{\lfloor\theta_j\cosh(\omega_2)-1\rfloor}{\sinh(\omega_2)}\sinh(m_2\tau) \tag{23b}$$

where,

$$m_1=\left(\frac{Bi}{\alpha\delta}\right)^{1/2} \tag{23c}$$

$$m_2 = \left(\frac{Bi}{\delta}\right)^{1/2} \quad (23d)$$

$$\omega_1 = m_1\lambda \quad (23e)$$

$$\omega_2 = -m_2(1-\lambda) \quad (23f)$$

$$z_1 = \sinh(\omega_1)\sinh(\omega_2) \quad (23g)$$

$$z_2 = \cosh(\omega_1)\cosh(\omega_2) \quad (23h)$$

$$z_3 = \cosh(\omega_1)\sinh(\omega_2) \quad (23i)$$

$$\theta_j = -\frac{m_2\cosh(\omega_1)}{m_1\alpha z_1 - m_2 z_2 + (1-\alpha)Biz_3} \quad (23j)$$

Table 1. The dimensionless tip temperature as a function of the number of terms in the series for α=0.5, Bi=0.1, δ=0.05 and λ=0.5

Number of terms in the series	β= -0.5	β= -0.3	β= -0.1	β= 0.0	β= 0.1	β= 0.3	β= 0.5
1	0.954364	0.965996	0.973051	0.975610	0.977734	0.981051	0.983517
2	0.399166	0.402534	0.405542	0.406952	0.408314	0.410926	0.413429
3	0.326187	0.346194	0.369117	0.381951	0.395905	0.428069	0.468286
4	0.302191	0.330720	0.363248	0.380992	0.399636	0.439031	0.479345
5	0.292559	0.325638	0.362055	0.380971	0.399939	0.436500	0.468683
6	0.288043	0.323730	0.361797	0.380971	0.399847	0.435895	0.469361
7	0.285744	0.322970	0.361738	0.380971	0.399836	0.436143	0.470689
8	0.284499	0.322653	0.361724	0.380971	0.399839	0.436197	0.470474
9	0.283793	0.322517	0.361720	0.380971	0.399839	0.436160	0.470095
10	0.283376	0.322457	0.361720	0.380971	0.399839	0.436157	0.470292

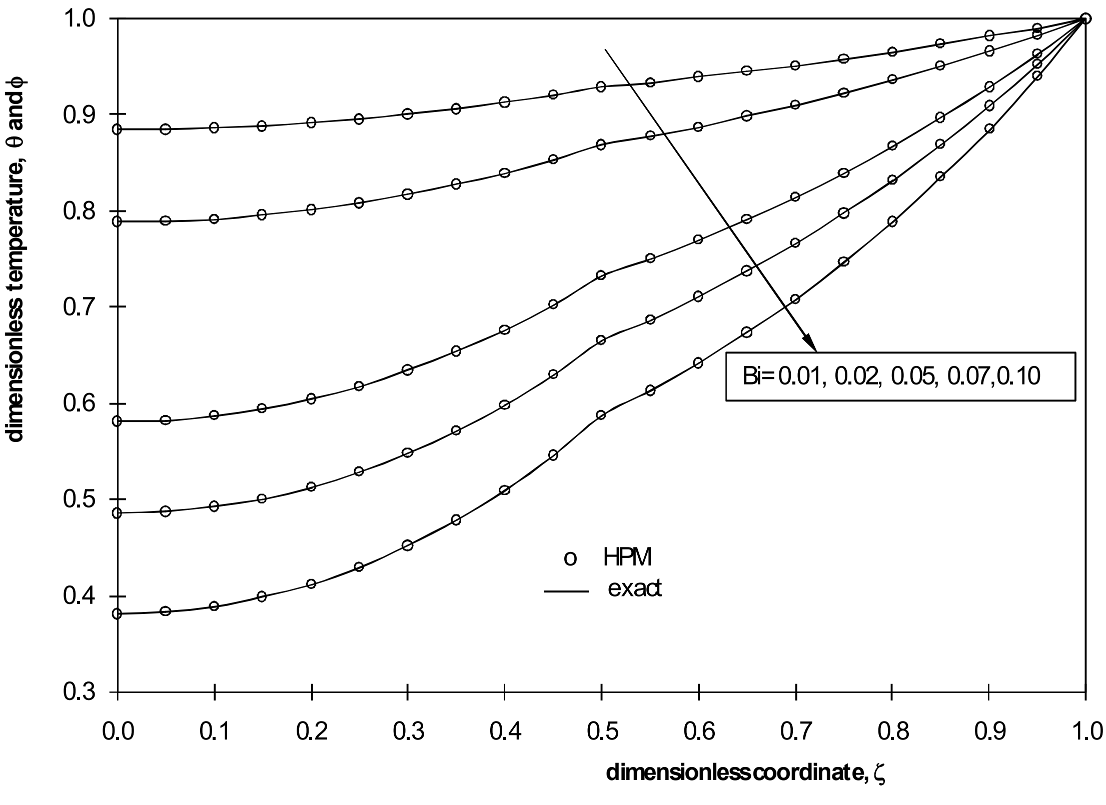

Figure 2.. The comparison of HPM and exact solution for the case of constant conductivity ,i.e, β=0.0 (λ=0.5, δ=0.05, α=0.5).

We take ten terms of approximate solution as our solution and compare it with the analytic solution which is the special case of β=0, and then we can realize that the results of both approximate and analytic solutions almost match (see Fig. 2).

In order to investigate the accuracy of the HPM solution with a finite number of terms, the problem is also solved numerically by using MAPLE which uses a finite difference method with Richardson extrapolation (Ascher and Petzold, 1998) and the corresponding results are compared with the HPM solution and presented in Table 2. The results of the comparison show that the maximum difference between HPM and numerical results for the strongest nonlinearity condition, i.e., Bi=0.10 and β=-0.5, is 0.25 %.

Table 2. Comparison of HPM and numerical solutions for different Bi and β (α=0.5, δ=0.05, and λ=0.5).

	Bi=0.01				Bi=0.10			
	tip temperature		junction temperature		tip temperature		junction temperature	
β	HPM	numerical	HPM	numerical	HPM	numerical	HPM	numerical
-0.5	0.80524	0.80477	0.87556	0.87513	0.28338	0.28266	0.47625	0.47500
-0.4	0.82743	0.82731	0.89124	0.89113	0.30276	0.30253	0.50120	0.50081
-0.3	0.84579	0.84573	0.90377	0.90371	0.32246	0.32239	0.52508	0.52497
-0.2	0.86100	0.86095	0.91387	0.91382	0.34217	0.34216	0.54753	0.54751
-0.1	0.87370	0.87366	0.92213	0.92209	0.36172	0.36171	0.56845	0.56843
0.0	0.88441	0.88433	0.92900	0.92892	0.38097	0.38096	0.58787	0.58785
0.1	0.89354	0.89347	0.93479	0.93472	0.39984	0.39982	0.60588	0.60585
0.2	0.90139	0.90133	0.93972	0.93966	0.41825	0.41823	0.62258	0.62254
0.3	0.90821	0.90816	0.94398	0.94392	0.43616	0.43613	0.63808	0.63804
0.4	0.91418	0.91413	0.94769	0.94763	0.45350	0.45348	0.65247	0.65244
0.5	0.91946	0.91935	0.95096	0.95085	0.47029	0.47024	0.66589	0.66585

OPTIMIZATION

The heat transfer rate from the fin is found by applying the Fourier law at the fin base.

$$Q = 2tk \left.\frac{dT_2}{dx_2}\right|_{x_2=L-\ell} \quad (24)$$

The objective here is to maximize the dimensionless heat transfer rate q, subject to the constraint that the dimensionless fin cross-sectional area is equal to a given value. The dimensionless heat transfer rate, i.e., the objective function, is written as follows

$$q = \frac{Q}{2k_\infty(T_b - T_\infty)} = (1+\beta)\delta \left.\frac{d\phi}{d\tau}\right|_{\tau=1-\lambda} \quad (25)$$

and the dimensionless cross-sectional area, i.e., equality constraint, of the step fin which is shown in Fig. 1 is

$$a = A_c/(2L^2) = \delta[1-\lambda(1-\alpha)] = \text{constant} \quad (26)$$

For a given value of the cross-sectional area, the dimensionless unreduced semi-thickness of the fin is expressed as:

$$\delta = \frac{a}{[1-\lambda(1-\alpha)]} \quad (27)$$

Substituting Eq.(27) into Eq(25), the objective function can be obtained as a function of fin length ratio λ and thickness parameter α, for given Biot number Bi, thermal conductivity parameter β and dimensionless cross-sectional area of the fin, a. The objective function is a very complicated expression and includes three unknown integral constants, C_1, C_2, and C_3. Since the values of the coefficients depend on the fin geometry, it is not convenient to use a classical optimization technique. For finding the optimal geometrical parameters which maximize the dimensionless heat transfer rate for given problem parameters a, β, and Bi, following procedure is applied.

Selecting values of α and λ, the temperature distribution within the fin is found as a function of integral constants

C_1, C_2, and C_3. Substituting fin temperature distribution to boundary conditions given Equations (3d), (3e), and (3f), the integral constants C_1, C_2, and C_3 are evaluated by classical Newton-Raphson method. The value of the objective function corresponding selected values of λ and α is obtained using Eq. (25). The values of λ and α are changed for many times in suitable intervals and corresponding dimensionless heat transfer rate, i.e., the objective function, is obtained. For every group of parameter, the value of the objective function is attained of an element of the array. The element with maximum value of the array is found by using a classical search method.

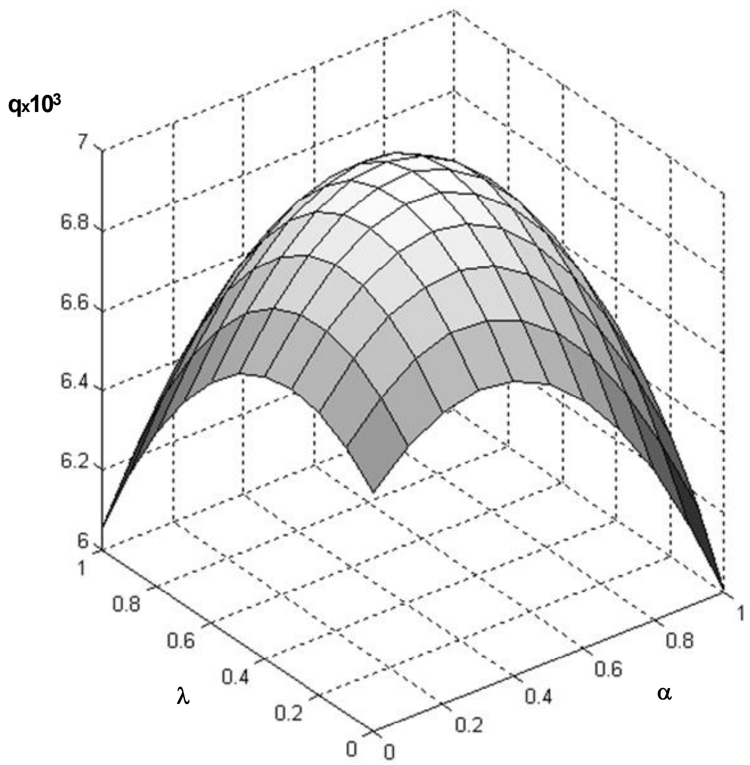

Figure 3. Dimensionless heat transfer rate as a function of fin length ratio and thickness parameter (a=0.005, Bi=0.01, β=0.2).

RESULTS AND DISCUSSION

The series solution for temperature distribution is evaluated by using homotopy perturbation method. This method gives a nearly analytical solution which is in the form of infinite series by computing the infinite terms. After getting the temperature distribution, dimensionless heat transfer rate for convective straight step fins is determined for a wide range of problem parameters from the present analysis. Fig. 3 is utilized for the presentation dimensionless heat transfer rate from convective step fin as a function of thickness parameter, α and fin length ratio, λ for β=0.2, a=0.005, and Bi=0.01. The figure states that the heat transfer rate has a maximum value for given thermal and geometrical parameters.

Fig. 4a shows the optimal values of length ratio and thickness parameter which maximize dimensionless heat transfer rate as a function of Biot number for a given constant cross-sectional area of the fin. From the figure, it is clear that an increase in Bi increases the optimal fin length ratio λ^*, and decreases the optimal thickness parameter α^*. The variation of thermal conductivity parameter on optimal fin geometry can also be seen from Fig. 4a. With the increase in β, the optimal fin length ratio λ^* increases and the optimal thickness parameter α^*decreases. Fig. 4b shows maximum values of the dimensionless heat transfer rate corresponding to the optimum geometrical parameters given in Fig. 4a.

Fig. 5 shows that for a given cross-sectional area, a higher rate of heat transfer is possible from a step fin compared to a constant thickness fin. Optimum geometrical parameters and maximum heat transfer rates for various combinations of thermal conductivity parameters are given in Table 3 to provide an open choice to the designer.

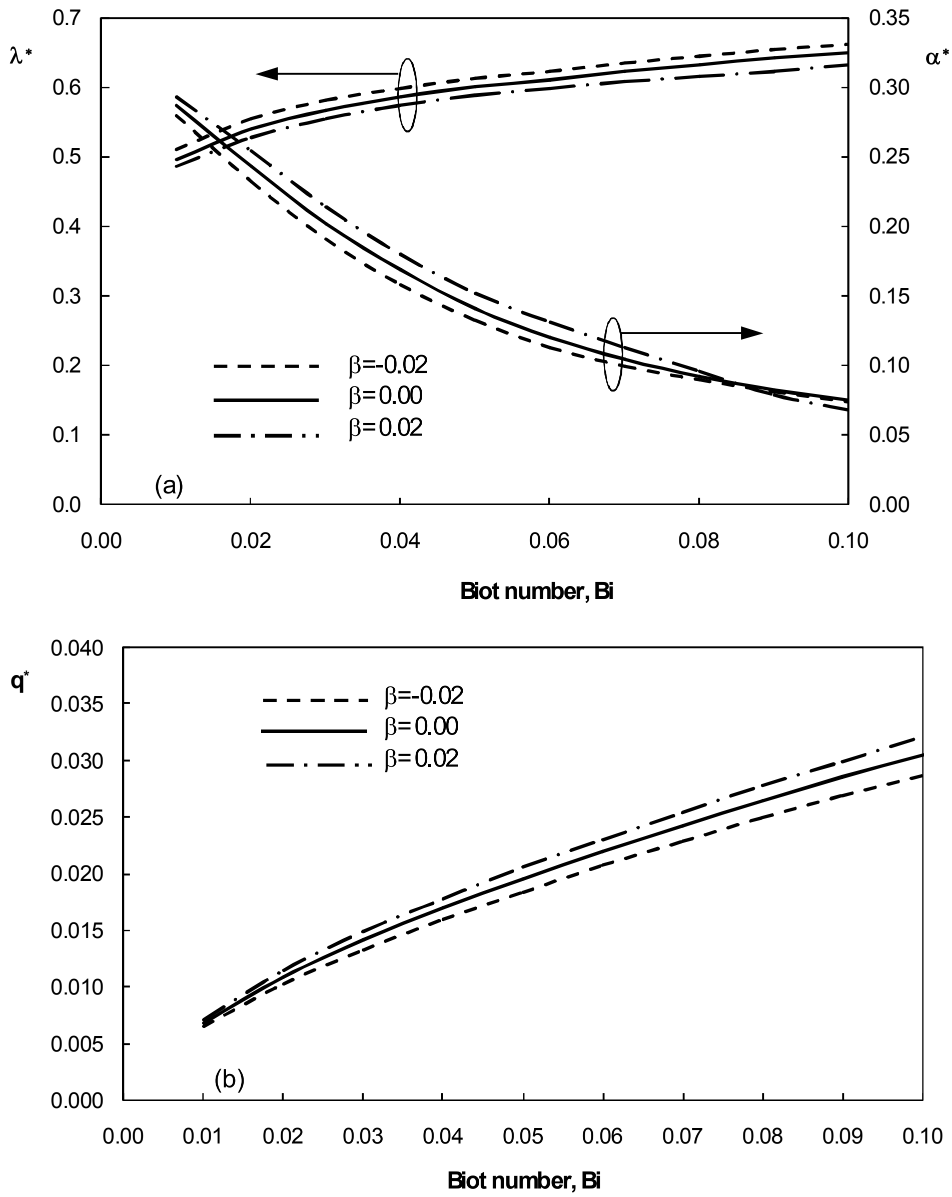

Figure 4. (a) Optimal fin length ratio and thickness parameter which maximize the dimensionless heat transfer rate. (b) Maximum dimensionless heat transfer rate as a function of conduction-radiation parameter (a=0.005).

Table 3. The optimum dimensions and maximum heat transfer rates of convective step fins for different thermal conductivity parameter.

	Bi=0.05						Bi=0.10					
	a=0.003			a=0.006			a=0.006			a=0.009		
β	λ^*	α^*	q^*	λ^*	α^*	q^*	λ^*	α^*	q^*	λ^*	α^*	q^*
-0.3	0.650	0.087	0.01474	0.614	0.150	0.01905	0.660	0.086	0.02967	0.642	0.118	0.03449
-0.2	0.640	0.086	0.01529	0.603	0.151	0.01974	0.651	0.086	0.03076	0.632	0.119	0.03573
-0.1	0.634	0.088	0.01578	0.597	0.157	0.02035	0.645	0.087	0.03174	0.627	0.123	0.03685
0.0	0.628	0.089	0.01623	0.590	0.162	0.02093	0.639	0.088	0.03264	0.620	0.127	0.03788
0.1	0.620	0.089	0.01665	0.584	0.168	0.02148	0.631	0.089	0.03348	0.613	0.132	0.03886
0.2	0.611	0.090	0.01704	0.579	0.174	0.02201	0.620	0.089	0.03426	0.607	0.139	0.03979
0.3	0.599	0.092	0.01741	0.576	0.179	0.02252	0.608	0.090	0.03499	0.605	0.147	0.04069

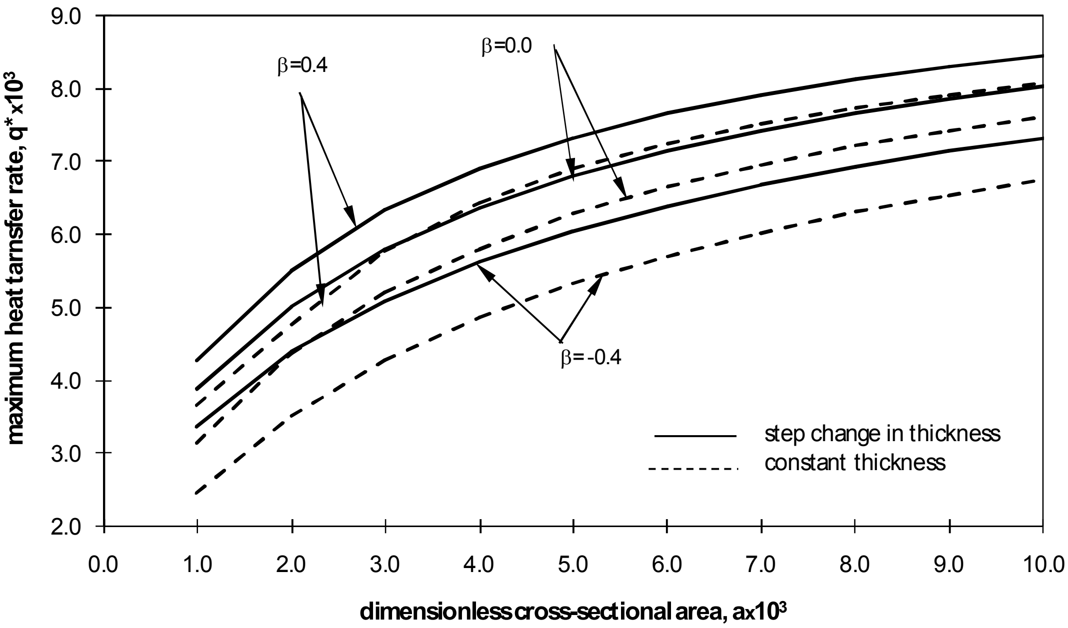

Figure 5. Variation of the maximum heat transfer rate with dimensionless cross-sectional area for Bi=0.01.

CONCLUSION

The present work is concentrated optimization analysis of convective straight step fins with temperature-dependent thermal conductivity. Since the fins have a step change in thickness, the fin problem has been divided into two parts as thin and thick sections. Resulting two nonlinear heat transfer equations with nonlinear boundary conditions have been solved by homotopy perturbation method to obtain the fin temperature distribution. The temperature profile has an abrupt change in the temperature gradient where the step change in thickness occurs and thermal conductivity parameter describing the variation of thermal conductivity has an important role on the temperature profile and the heat transfer rate. The optimum geometry which maximizes the heat transfer rate for a given fin cross-sectional area has been found. The results demonstrated that the maximum heat transfer rate is always higher for a step fin than that of a constant thickness fin for the identical design condition.

REFERENCES

Ascher, U., and Petzold, L., *Computer methods for ordinary differential equations and differential-algebraic equations,* SIAM, Philadelphia, 1998.

Aziz, A., Optimum design of a rectangular fin with a step change in cross-sectional area, *International Communications in Heat and Mass Transfer,* 21, 389-401, 1994.

Cowdhury, M. S. H., and Hashim, I., Analytical solutions to heat transfer equations by homotopy-perturbation method revisited, *Physics Letters A*, 372, 1240-1243, 2008.

Cowdhury, M. S. H., Hashim, I., and Abdulaziz, O., Comparison of homotopy analysis method and homotopy-perturbation method for purely nonlinear fin-type problems, *Communications in Nonlinear Science and Numerical Simulation*, 14, 371-378, 2009.

He, J. H., Homotopy perturbation technique, *Computational Methods in Applied Mechanics and Engineering,* 178, 257-262, 1999.

He, J. H., A coupling method of a homotopy technique and a perturbation technique for non-linear problems, *International Journal of Non-Linear Mechanics,* 35, 37-43, 2000.

He, J. H., Homotopy perturbation method: A new nonlinear analytical technique, *Applied Mathematics and Computation* 135, 73–79, 2003.

Hollands, K. G. T., and Stedman, B. A., Optimization of an absorber plate fin having a step change in local thickness, *Solar Energy* 49, 493-495, 1992.

Kern, Q. D., and Kraus, D. A., *Extended Surface Heat Transfer*, McGraw-Hill, New York, 1972.

Kundu, B., and Das, P. K., Performance analysis and optimization of annular fin with a step change in thickness, *Journal of Heat Transfer*, 123 601-604, 2001.

Kundu, B., and Das, P. K., Performance analysis and optimization of straight taper fins with variable heat transfer coefficient, *International Journal of Heat and Mass Transfer*, 45, 4739-4751, 2002.

Kundu, B., and Das, P. K., Performance analysis and optimization of elliptic fins circumscribing a circular tube, *International Journal of Heat and Mass Transfer*, 50, 173-180, 2007.

Kundu, B., Analysis of thermal performance and optimization of concentric circular fins under dehumidifying conditions, *International Journal of Heat and Mass Transfer*, 2646-2659, 2009.

Malekzadeh P., Rahideh, H., and Karami, G., Optimization of convective-radiative fins by using differential quadrature method, *Energy Conversion and Management,* 47, 1505-1514, 2006.

Öziş, T., and Ağırseven, D., He's homotopy perturbation method for solving heat-like and wave-like equations with variable coefficients, *Physics Letters A,* 372, 5944-5950, 2008.

Saadatmandi, A., Dehghan, M., and Eftekhari, A., Application of He's homotopy perturbation method for nonlinear system of second-order boundary value problems, *Nonlinear Analysis: Real World Applications,* 10, 1912-1922, 2009.